

Trivent Publishing

© The Authors, 2016

Available online at <http://trivent-publishing.eu/>



Engineering and Industry Series

Volume Power Systems, Energy Markets and Renewable Energy Sources in South-Eastern Europe

An Experimental Evaluation of a Flexible Wind Turbine Rotor

C. Condaxakis,¹ I. Kougioumtzoglou,² N. Papadakis¹

¹ Wind Energy & Power System Synthesis Laboratory – TEI of Crete, Estavromenos, 71004 Heraklion, PO Box: 1939, Greece, tel: 0030 2810256191, condax@cs.teicrete.gr

² School of Engineering, Interdepartmental Postgraduate Programme “Energy Systems” – TEI of Crete, Greece, kugiumtzog@hotmail.com

Abstract

This paper studies the design concept of a flexible wind turbine blade. The aim of the blade structural design is to optimize the geometrical and inertial property distribution for each cross section of the blade; furthermore, its aim is to effectively control the wind rotor and reduce the aerodynamic loads on the blade.

Due to its design, the blade achieves a deformed geometry that satisfies the optimisation criteria in a wide range of aerodynamic load conditions. The aerodynamically-induced bending moment coupled with the eccentricity between the elastic and aerodynamic centre of each blade cross-section results in a deformation. The deformation increases with the load. The resulting deformation is bending and twisting, and results in the change of the pitch along the blade, depending on the aerodynamic loads. The Solidworks commercial package was used for the structural blade design and the Finite Element analysis of the blade. Small-scale models (320 mm rotor diameter) were designed, manufactured and tested in the Wind Energy Lab’s wind tunnel. The behavior of the miniature rotors was compared to the behavior of equal diameter conventionally-shaped rigid rotors.

Keywords

Flexible wind blade; Passive control blade; adaptive blade

This is an Open Access article distributed in accordance with the Creative Commons Attribution Non Commercial (CC-BY-NC-ND 4.0) license, which permits others to copy or share the article, provided original work is properly cited and that this is not done for commercial purposes. Users may not remix, transform, or build upon the material and may not distribute the modified material (<http://creativecommons.org/licenses/by-nc/4.0/>)

DOI: 10.22618/TP.EI.20163.389022

I. Introduction

The growth of the wind energy industry over the last decades has made the reduction of the cost of energy (COE) necessary and has opened a new field of research. One option is to reduce or eliminate all the component parts involved in the pitch and stall system function of the horizontal axis wind turbines (HAWT). To achieve that, curved geometry blades should be designed and constructed in order to minimize the rotor's torque in high wind speeds. This can be attained by the variation of the twisting angle (pitch angle) at the outboard region of the wing; this results in the stall condition in the blade.

Larwood S. and M. Zuteck [1] show that the swept-blade concept was used in order to increase energy capture without an increase in the turbine loads. They studied a 56 meter backward swept blade (STAR6) in comparison to a straight-rigid blade rotor (50 meters), showing that the swept blade rotor created a 5-10% increased energy capture without increasing the load envelope.

"Knight & Carver" was contracted by Sandia National Laboratories [2] to develop a sweep-twist adaptive blade (STAR) that reduced operating loads, thereby developing a larger, more productive rotor. The passive blade twist in the outer blade used to limit the maximum rotor thrust. The tests have shown that a 54 m backward-swept prototype blade (termed the STAR blade) can increase the average energy capture by 10–12% compared to a 48 m straight-rigid-bladed rotor diameter without increasing the blade root bending moments.

M. Zuteck [3] proposed a bend-twist coupling for blades, for passive control of the rotor, with the ability to self-adjust its geometry according to the aerodynamic loads. Zuteck found that lowering the torsion stiffness would be necessary to obtain sufficient twisting; on the order of 5° . He also proposed increasing the rotor diameter so as to reduce the cost of energy. In addition, in a similar study as the previously-mentioned one, M. Capuzzi [4] proposed an aero-elastically tailored blade, analyzed by using finite element models with structural stability and strength constraints imposed under realistic load cases.

Larwood's [5] paper describes a parametric study of swept blade design parameters for a 750 kW machine. The amount of tip sweep had the largest effect on the energy production and blade loads; other parameters had less impact. The authors then conducted a design study to implement a swept design on 1.5 MW, 3 MW, and 5 MW turbines. An aeroelastic code, described in the paper, was developed to model the behavior and determine the loads of the swept blade. The design's goal was to increase annual energy production 5% over the straight-rigid blade, without increasing blade loads.

Xin Shen [6] describes a multi-objective optimization method for the design of horizontal axis wind turbines using the lifting surface method as the performance prediction model. The purpose of the optimization method is to achieve the best trade off of the following objectives: maximum annual energy production and minimum blade loads including thrust and blade root flap-wise moment. The result shows that the optimization models can provide more efficient designs.

M.G. Khalafallah [7] presented a CFD simulation of a swept blade HAWT for a 0.9 m diameter wind turbine model. Four different scenarios were simulated, a backward sweep, a forward sweep, an upstream sweep and a downstream sweep blade compared to a straight-rigid blade. The results show that the downstream swept blades are able to generate more output power than the straight-rigid blades but with a relatively higher axial thrust force. So the blade deflection and tower clearance should be considered during the design phase of swept blades rotors.

This paper presents the design of a small rotor (0.32 meters diameter) with curved geometry blades which was designed and printed initially in a 3D printer with ABS material and then constructed in a CNC machine using HDPE material. The blades have a forward swept design and the sweep starts at 20% of the span axis (0.2 r/R). Numerical analysis of blade's static load cases were carried out for the design. Static experiments were also carried out to validate the design and the numerical result. This rotor was tested in a wind tunnel and the results were compared to a matching diameter straight-rigid blade rotor.

II. Design process

For the blade design, calculations were made using mathematical models. For the aerodynamic model, DEOL program was used, a simple aerodynamic code based on the Glauert theory for airfoil and airscrews improved by researchers at AMHERST, described in 'Les Eoliennes', of Désiré Le Gourières [8]. DEOL calculates the axial lift component force in the rotor plane, while the theory of bending was used for the elastic model. The elastic behavior of the material was simulated with the appropriate use of spring and dampening elements (see fig1.).

As shown in fig.1, the angle that formed between the resultant wind speed (W_2) and the Chord, the angle of attack (i), is greater than the one in the second sketch. Furthermore the pitch angle ($\alpha' - \alpha$), as shown in the second sketch, is changing. This happens due to the wind speed (V_2) which is much higher than (V_1), which results in producing much higher lift force. All the above lead to the bending deformation (h) and twisting deformation of the blade ($\alpha' - \alpha$). For high wind speeds, the value of the attack angle (i) becomes higher causing the blade to enter in the aerodynamic stall area.

In order to calculate the aero-elastic model, a straight-rigid blade was initially designed by using the geometry calculated by DEOL program composed by 10 airfoil profiles, along the blade. All the geometric parameters i.e. the chord, the pitch angle and the airfoil type for each of the 10 sections were already known as they had been prior calculated. Based on the geometry of the straight-rigid, a curved geometry blade was designed.

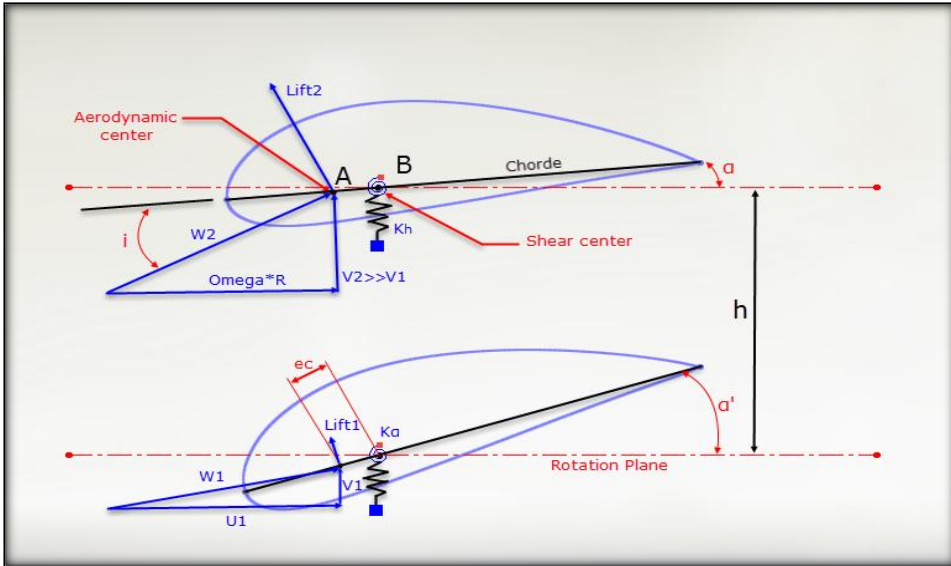


Fig. 1. Blade section deformations due to aerodynamic loads. A: axis of aerodynamic centers, B: elastic axis, α : pitch angle, $\alpha' - \alpha$: pitch angle change due to elastic deformation, h : bending deformation, ec : elastic-aerodynamic eccentricity.

For a straight-rigid blade, the aerodynamic loads lay near the blade elastic axis at all spanwise sections. On a blade with an eccentric elastic axis, the loads are in an offset distance from the elastic axis of the theoretical straight-rigid blade. It is possible to calculate the torsional moment distribution along the blade from the offset distances imposed by the blade's planform curve, given the eccentricity and the spanwise loading distribution. Therefore, an adequately flexible blade bends and twists under the aerodynamic excitation.

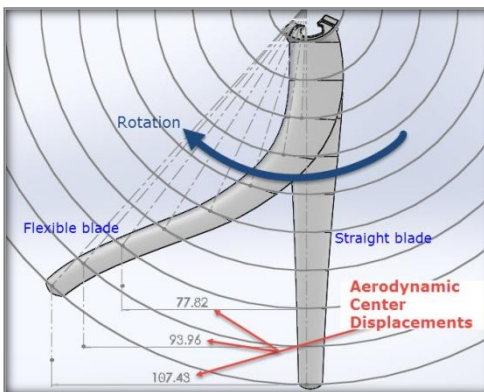


Fig. 2. Aerodynamic center displacements.

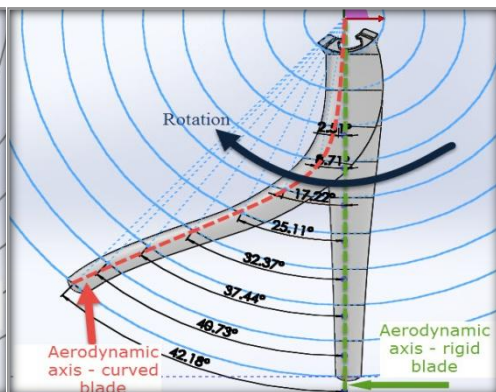


Fig. 3. Aerodynamic axis.

Table 1. The geometrical characteristics of the rigid blade and the eccentricity of the flexible one.

RIGID BLADE					FLEXIBLE BLADE			
SECTION	RADIUS (m)	CHORD (m)	<i>i</i> (angle of attack)	<i>a</i> (setting angle)	AERODYNAMIC CENTER DISPLACEMENTS (m)	CURVATIVE ANGLE (deg)	<i>a</i> (setting angle)	SURFACE APPLYING PRESSURE (mm ²)
1	0.016	0.0238	15.811	27.095	0.00000	0.00	27.15	-
2	0.032	0.0242	11.180	19.599	0.00000	0.00	20.21	396.26
3	0.048	0.0227	9.129	14.057	0.00210	2.51	15.50	389.25
4	0.064	0.0202	7.906	10.436	0.00969	8.71	13.13	361.24
5	0.080	0.0177	7.071	8.009	0.02368	17.22	13.82	322.45
6	0.096	0.0156	6.455	6.310	0.04074	25.11	15.63	284.14
7	0.112	0.0138	5.976	5.073	0.05969	32.37	17.72	251.26
8	0.128	0.0123	5.590	4.141	0.07782	37.44	17.31	219.66
9	0.144	0.0111	5.270	3.418	0.09396	40.73	15.80	193.55
10	0.160	0.0101	5.000	2.846	0.10743	42.18	15.00	172.95

In the current project, in order to design the curved blade, the research indicated that the sweep should start from the 3rd section (from 0.2 r/R of spanwise axis, see Table 1). The geometric parameters of each section are the same in the straight-rigid and the flexible blade. The differences between a straight-rigid and a flexible blade are regarding the setting angle and the angle of rotation around the rotor axis (see fig. 2 and 3). The chord length remains unchanged while sliding, and always tangent to the circle defined by the rigid straight-rigid rotor cross sections. The curved blade geometry is designed to create an 11.8° twist towards stall (see fig. 1 α' - α) at the blade tip, at a wind speed of 16 [m/sec], compared to the rigid blade.

The parametric design was implemented by using excel spreadsheets. The results which were obtained, refer to the number and all the geometric parameters of airfoils (such as chord length, angle of attack, pitch angle and thickness ratio $\delta\%$) by entering some basic data such as the radius R of the blade and the speed ratio λ_0 . The calculations were made based on the classic Glauert airscrews theory, described in LES EOLIENNES of D. Le Gourières [8] and by using a Naca4415 airfoil. The coordinates (x,y,z) of each airfoil profile can be calculated for a straight-rigid or a curved blade by entering the curving angle for each section. The Solidworks commercial package was used for the structural blade design and the Finite Element Analysis (FEA) of the blade.

III. Construction process

A very important parameter, for the blades, is the construction material. High Density Polyethylene (HDPE) material was selected because of its mechanical properties (800 N/mm^2 of elastic modulus and 30 N/mm^2 of tensile strength). The selection of HPDE was validated through Finite Elements Analysis. For the construction of the blades, a two axis CNC machine was used in order to have a solid structure. After the construction of the blades, a hub was designed and constructed in a 3D printer using ABS material and afterwards the rotor was assembled.

IV. Experimental procedure

Once the rotor was completed, it was tested statically using weights simulating the aerodynamic loads, in order

- To measure the deformations regarding the displacement and angle along the blade and compare them to the corresponding calculated values.
- To ensure the strength of the blade under the loads.

The comparative results are in compliance to the expected behavior for both the straight and the curved blade.

After the static tests the rotor was tested in the wind tunnel. After verifying its balance, the rotor was placed in a fully instrumented wind tunnel at the Wind Laboratory of TEI Crete. A SCAIME model No DR2112L with embodied encoder torque meter with capability of measuring 1 [Nm] was used. In order for the drag force to be measured, a load cell (HBM model No SP4MC6MR) was been placed at the measuring device (see fig. 4).

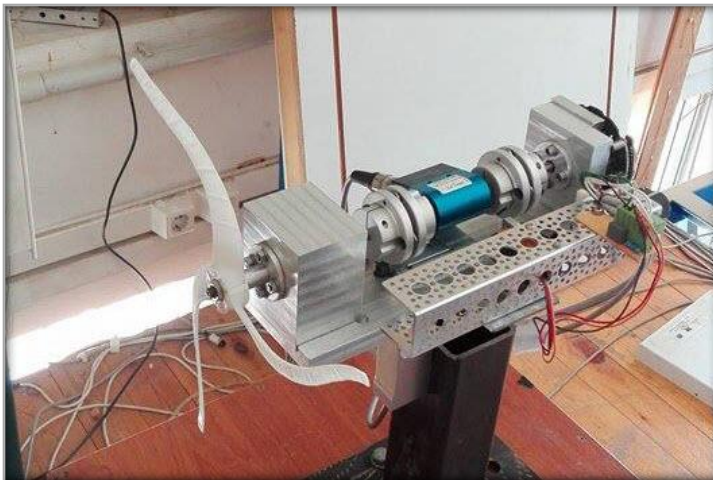


Fig. 4. Measuring device in front of wind tunnel.

The rotational speed, torque, and drag force were measured at different wind speed velocities. The wind speed at the wind tunnel outlet was measured with a Pitot-Prandtl tube and a Delta Ohm HD408T differential pressure transducer. The data acquisition system was built upon Labview 8.6 Development System.

V. Measurements Procedure

When the rotor was tested in the wind tunnel, two sets of measurements were carried out to improve the accuracy of the results. If the measurements were not relatively identical (difference $> 1\%$) they would be rejected and repeated. The measurements' sampling rate was 100ms.

Four different sets of tests were conducted for both the straight-rigid and the curved rotor:

- The first test was without applying any load to the rotor.
- The second test was conducted applying a small load using a constant mechanical brake to the rotor axis
- The third test was conducted applying a bigger load using a constant mechanical brake to the rotor axis and
- The last test was with constant wind speed and variable load.

The torque measurements were accomplished with the use of brake in every wind speed from 4-19 [m/sec].

VI. Measurement Post-Processing

The data were stored in ASCII format. The analysis was carried out using Labview and Excel (.xls).

Fig. 5 presents a graph of Rotational speed versus the wind speed velocity. Three regions can be observed with respect to the wind speed:

- up to 4[m/s]: Rotational velocity is zero for the curved blade and up to 6[m/s] for the straight-rigid blade.
- 4[m/s] - 16[m/s]: The rotational velocity increases almost linearly from zero up to approximately 2750[rpm] for the curved blade and up to 7000[rpm] for the straight-rigid blade.
- 16[m/s] - 19[m/s]: The rotational velocity reaches a plateau between 2500 and 3000[rpm] for the curved blade. The straight-rigid blade broke at wind speed 16[m/s] so it was impossible to observe its behavior at this wind speed range.
- For the Drag measurements a linear continuous increase is observed for the straight-rigid blade that results in the blade failing, while in the measurements of the curved blade, an increase much lower (about 30% of the drag) in comparison to the rigid blade, is observed.

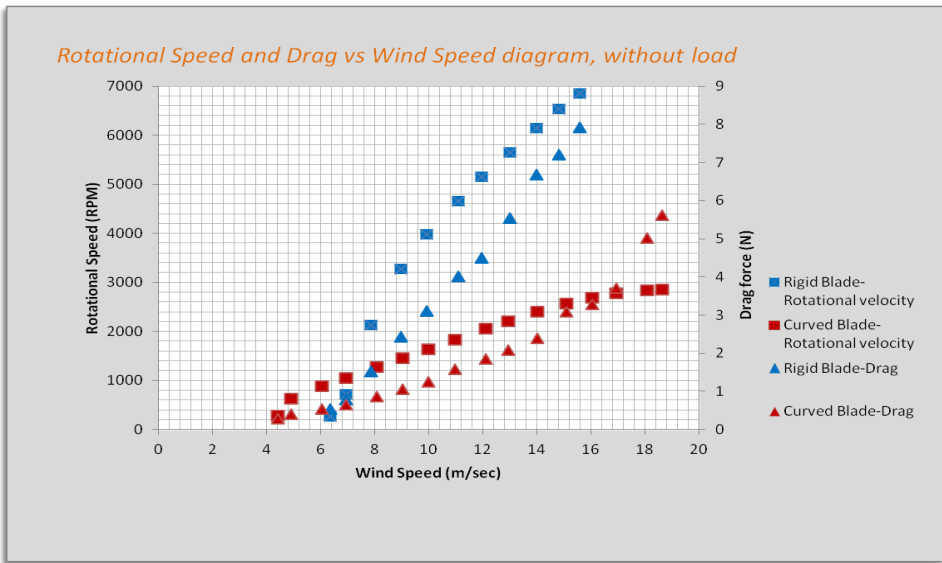


Fig. 5. Rotational speed and Drag vs. Wind speed diagram, without load, 1m/s bins.

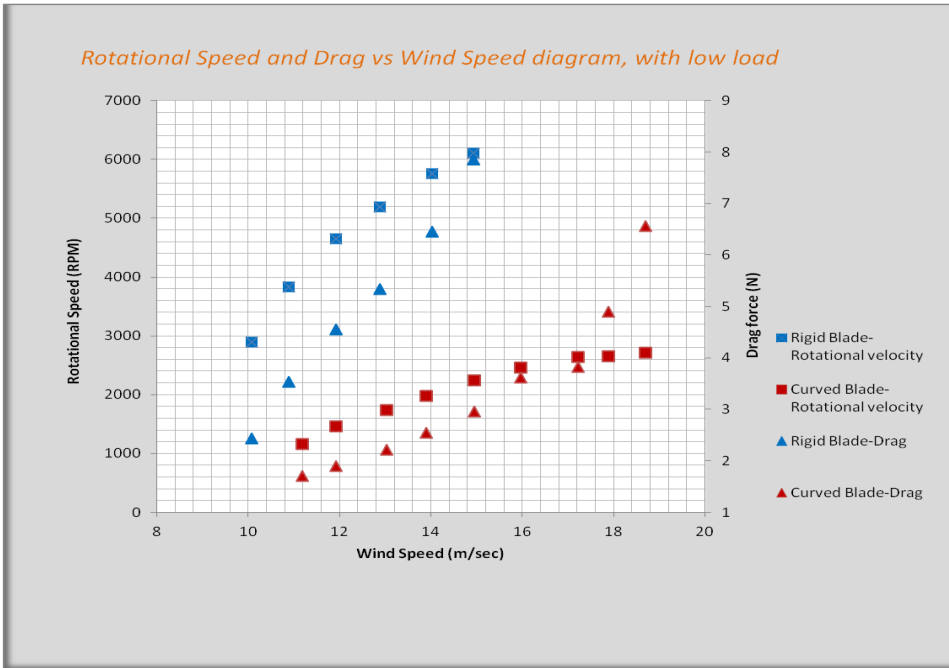


Fig. 6. Rotational speed and Drag vs. Wind speed diagram, with low load, 1m/s bins.

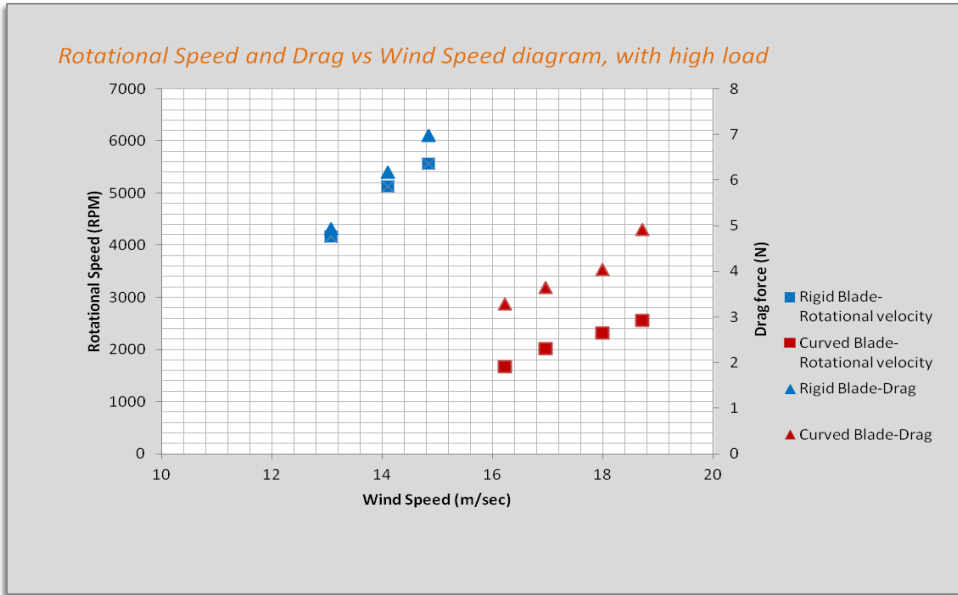


Fig. 7. Rotational speed and Drag vs. Wind speed diagram, with high load, 1m/s bins.

The same behavior is observed from the measurements with a load, low or high, figures 6 and 7. Both the rotational speed and the Drag forces are about three times higher for the same wind speed in the case of the straight-rigid rotor.

The extracted mechanical power is a calculated quantity from n , the rotor rotational velocity in RPM and Torque in Nm:

$$P[W] = \frac{2 \cdot \pi}{60} \cdot n[\text{rpm}] \cdot \text{Torque}[\text{Nm}]$$

The different colors, red and black, in the following graphs concern different sets of measurements, without any load.

In the case of the straight rigid rotor, the Power increases constantly due to the absence of a control system (see fig. 8). In the case of the flexible-curved rotor (see fig. 9, 10) the Power is limited presenting a behavior similar to the presence of a control system.

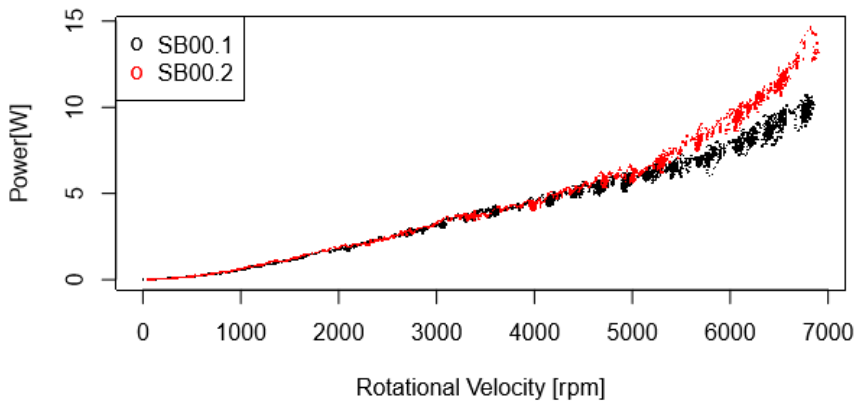


Fig. 8. Power scatter vs. wind speed for the straight rigid rotor.

It is interesting to note the difference between the following plots for the curved blade (see fig. 9, 10):

- Power vs rpm
- Power vs Wind Speed

In Power vs Wind Speed the curved blade beyond 15[m/s] produces power steadily around 2.5[W]. This is presented in the Rotational Velocity graph as a big blob of data around 2.5[W] and 2700[rpm]. The Rotational Velocity graph is misleading with respect to the performance and range of wind speed (in most blades rotational velocity is more or less proportional up to breaking). In the Power curve in fig. 10, the flexible rotor seems to achieve an effective control passively, similar to the rotors with an active pitch or stall control, using complex and expensive servo hydraulic systems.

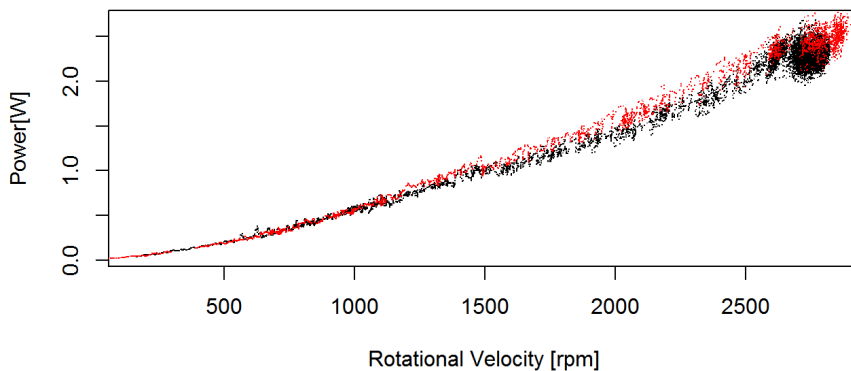


Fig. 9. Power scatter vs. rotational velocity for the curved blade rotor.

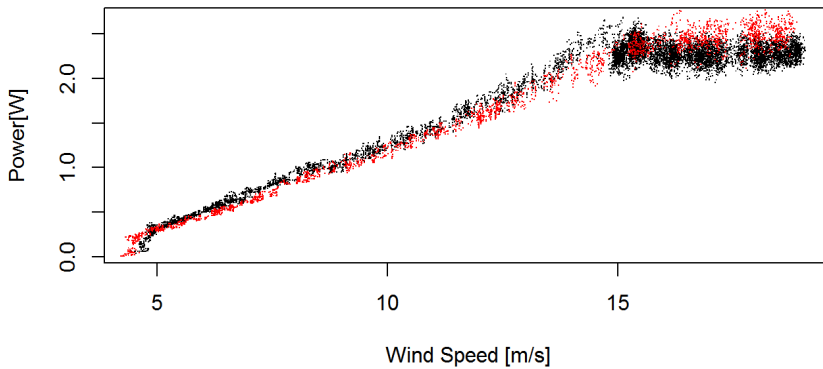


Fig. 10. Power scatter vs. wind speed for the curved blade rotor.

VII. Conclusions

A rotor, whose blades have great elasticity due to their curved geometry, was calculated, designed and constructed. This particular geometry was designed so as to give to the blade the ability of torsional deformation, meaning the change of the pitch angle according to the aerodynamic loads that are being applied on it. The blade was statically tested and afterwards it was tested in the TEI of Crete, Wind Energy Lab Wind Tunnel in order for its behavior to be examined in comparison to a straight-rigid blade of the same geometry and size. The first results from the measurements have shown that the blade is being deformed in order to maintain its rotational velocity stable over a certain wind speed, keeping also the loads that are being applied on it at much lower levels in comparison to a conventionally designed blade. It seems that there is the possibility of optimizing the curved blade design in order for a passively self-controlled rotor to be constructed.

References

- [1] Larwood, S., and M. Zuteck 2006. *Swept Wind Turbine Blade Aeroelastic Modeling for Loads and Dynamic Behavior*. Pittsburgh: AWEA Windpower.
- [2] Knight & Carver Wind Group, *Sweep-Twist Adaptive Rotor Blade: Final Project Report*. SANDIA REPORT SAND2009-8037 Unlimited Release, Printed January 2010
- [3] Mike Zuteck, *Adaptive Blade Concept Assessment: Curved Planform Induced Twist Investigation*. SAND2002-2996 Unlimited Release Printed October 2002.
- [4] M. Capuzzi, A. Pirrera, P.M. Weaver, *Structural design of a novel aeroelastically tailored wind turbine blade*. Advanced Composites Centre for Innovation and Science, Department of Aerospace Engineering, University of Bristol, Queen's Building, University Walk, 2015

- [5] Scott Larwood, C.P. van Dam, Daniel Schow, *Design studies of swept wind turbine blade* 2014
- [6] Xin Shen, Jin-Ge Chen, Xiao-Cheng Zhu, Peng-Yin Liu, Zhao-Hui Du, *Multi-objective optimization of wind turbine blades using lifting surface method*. Shanghai Jiaotong University 2015.
- [7] M.G. Khalafallah, A.M. Ahmed & M.K. Emam (2015): *CFD study of some factors affecting performance of HAWT with swept blades*. International Journal of Sustainable Energy, DOI: 10.1080/14786451.2015.1053394.
- [8] Désiré Le Gourières, *Les Éoliennes Théorie, conception et calcul pratique*, 2008, Éditions du Moulin Cadiou, ISBN13 : 978-2-953004-10-6

Acknowledgement

The current project has been supported by the 1st Internal Research Support Program which was funded by the Specific Account for Research and Funds (ELKE) TEI of Crete.